Evapotranspiration estimate from water balance closure using satellite data for the Upper Yangtze River basin

C. Corbari, M. Mancini, Z. Su and J. Li

ABSTRACT

Application of hydrological models for water resources management at large continental river basins is often limited by the scarcity of *in situ* meteorological forcing data. Remote sensing information provides an alternative to *in situ* data, with observations that are, in some cases, at higher spatial and temporal resolutions than those available from traditional ground sources. In this work, the water balance equation is solved using precipitation retrieved from Tropical Rainfall Measuring Mission, water storage from Gravity Recovery and Climate Experiment satellite data and ground discharge. Evapotranspiration (ET) is then computed as a residual term of the water balance. Satellite data are compared with ground data to understand to what extent remote sensing observations can be used to improve estimates of the terrestrial water balance at regional scale. ET estimates are also compared with the ET computed from a detailed distributed energy water balance model and with the ET product from the Moderate Resolution Imaging Spectroradiometer Global Evapotranspiration Project. These analyses are performed for the Upper Yangtze River basin (China) in the framework of NRSCC-ESA DRAGON-2 Programme.

Key words | evapotranspiration, remote sensing, water balance

C. Corbari (corresponding author)
M. Mancini
Politecnico di Milano,
Piazza Leonardo da Vinci 32,
20133, Milano,
Italy
E-mail: *chiara.corbari@polimi.it*

Z. Su
University of Twente,
Hengelosestraat 99,
7514 AE Enschede,
The Netherlands

J. Li
China Institute of Water Resources and Hydropower Research,
5 Summer Palace Road,
Beijing,
China

INTRODUCTION

Evapotranspiration (ET) is one of the main components of the water cycle and it is important in a wide range of applications from hydrology, to ecology, climate change and water resources management. Its quantification over large scales is a difficult task, in particular using distributed hydrological models which require a multitude of input information. However, these analyses are often limited by the scarcity of *in situ* meteorological forcing data in different regions of the world (Pan & Wood 2006). Nevertheless, in the last years there has been a wide diffusion of land surface models which compute mass and energy fluxes from regional to continental scales with reasonable results (Norman *et al.* 1995; Anderson *et al.* 1997; Bastiaanssen *et al.* 1998; Su 2002; Crow *et al.* 2003; Corbari *et al.* 2013).

Remote sensing information can provide an alternative to *in situ* data, with observations that are, in some cases, at higher spatial and temporal resolutions than those available from traditional surface sources. In particular in the last few years, there has been an improvement in availability and quality of satellite products for all the main variables of the water cycle (McCabe *et al.* 2008), so that closing the water budget seems to be feasible in areas with poor ground information (Rodell *et al.* 2004; Ramillien *et al.* 2006; Sheffield *et al.* 2009).

Moreover, satellite data take into account water irrigation information and also the effects of human presence on the water cycle which are not easily simulated with land surface models (Oki & Kanae 2006; Gao *et al.* 2010).

Precipitation information can be retrieved from different sensors using microwave and infrared data, such as Tropical Rainfall Measuring Mission (TRMM) or Advanced Microwave Scanning Radiometer (AMSR-E) (Adler *et al.* 2007; Huffman *et al.* 2007). Huffman *et al.* (2007) demonstrate good agreement between satellite and ground data, especially at temporal scales higher than daily. Li *et al.*

doi: 10.2166/nh.2013.016

(2012) used TRMM data for streamflow simulations in the Yangtze River basin, reporting good results at monthly scale.

Water storage can now be inferred from gravity changes from the Gravity Recovery and Climate Experiment satellite data (GRACE) (Swenson & Wahr 2002; Tapley *et al.* 2004). Discharge data can be retrieved from altimetry measurements, such as ERS-1 & 2, ENVISAT and Jason-1 (Birkett 1998; Frappart *et al.* 2006), even though two major problems should be raised: (1) only rivers with a sufficient width can be considered (approximately 350 meters) and (2) a poor temporal resolution is available with a range between 10 and 35 days, so that time series should be created from the interpolation of instantaneous measurements (Roux *et al.* 2008).

Global estimates of ET are now becoming possible, even though the implemented models still require additional ground information (e.g., wind speed, radiation) (Su 2002; Gao *et al.* 2010). Nevertheless in the last years, an ET product from the Moderate Resolution Imaging Spectroradiometer (MODIS) Global Evapotranspiration Project has become available (Mu *et al.* 2011). Moreover, in the literature, some scientific papers are available on the estimate of ET based only on the closure of the water balance. For example, Rodell *et al.* (2004) report that for the Mississippi River basin the ET computed from the European Center for Medium Range Weather Forecasting reanalysis is comparable to the residual ET estimated from the water balance closure using satellite data. In addition, Ramillien *et al.* (2006) found good agreement between the residual ET computed from the water balance and the ET estimated from different global land surface models for some large basins, including also the Yangtze River basin. Also, Moiwo *et al.* (2011) computed ET for another Chinese basin based on GRACE data.

However, Gao *et al.* (2010) state that closing the water budget based only on satellite data is not possible due to as yet high uncertainties in remote sensing data.

Jiménez *et al.* (2011) compared 12 global estimates of land surface heat fluxes at monthly scale from different satellite products and reanalysis models showing an overall mean difference of only 45 W m^{-2} on global latent heat fluxes, but with high discrepancies among different models, vegetations coverage and seasons.

The objective of this work is then to estimate ET from the simplified procedure of the closure of the water balance equation using ground and satellite data in order to understand to what extent remote sensing observations can be used to improve estimates of the terrestrial water balance at regional to continental scales and if they are able to better represent the variability of water cycle components in space and time compared to an operational hydrological model. The water balance will be solved using precipitation data retrieved from TRMM and from rain gauges, water storage from GRACE satellite and discharge data from ground stations. ET estimates are evaluated by comparison with the outputs of a distributed energy water balance model, Flash-flood Event-based Spatially-distributed rainfall–runoff Transformation–Energy Water Balance model (FEST-EWB). Then, a comparison with the ET estimates from MODIS is also computed.

These analyses are performed for the Upper Yangtze River basin (China) with an extent of about 1,000,000 km^2 in the framework of the NRSCC-ESA DRAGON-2 Programme.

STUDY AREA AND DATA

Study area

The test area is the Upper Yangtze River basin in China closed at Yichang (30.66 N, 111.23 E) where the Three Gorges dam is located. The total area is about 1,005,500 km^2 (Figure 1). The main river length is equal to 2,400 km with an average discharge of 13,242 m^3 s^{-1} and a mean annual precipitation of 800 mm concentrated during the monsoon period. This catchment drains a region characterised by 60% of mountains higher than 1,000 m a.s.l. and 40% of agricultural plain.

Satellite data

TRMM precipitation

The TMPA 3B42-RT product has been selected as satellite precipitation data (Huffman *et al.* 2007). This operative product is a combination of microwave and infrared data. In particular, it comes from the TRMM Microwave imager (TMI) and the Precipitation Radar (PR) data with

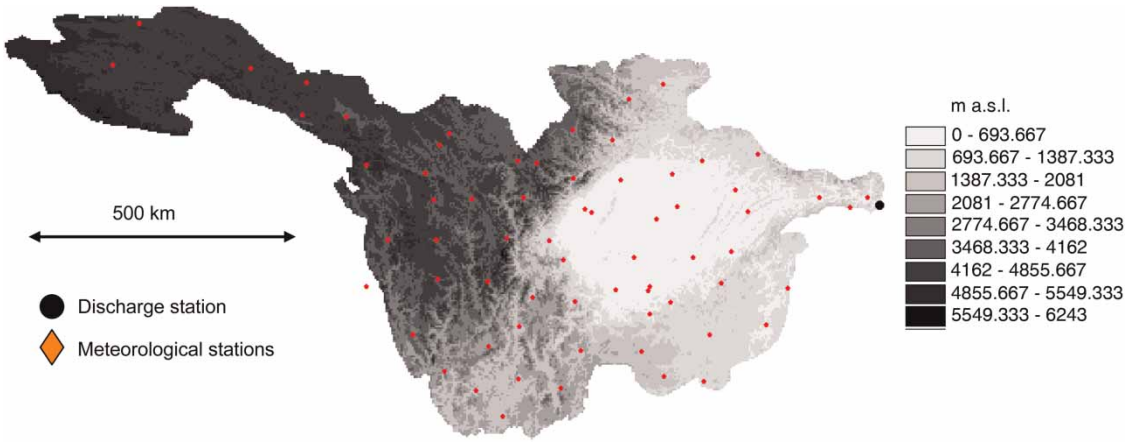

Figure 1 | Upper Yangtze River basin: digital elevation model, rain and discharge gauges.

corrections from the infrared data. The products are downloadable from http://trmmopen.gsfc.nasa.gov. The spatial resolution is characterised by a regular grid of 0.25° with a temporal resolution of 3 hours. The gridded products have been cumulated to monthly scale.

GRACE water storage

GRACE, launched in 2002, measures Earth's gravity field. Ground and surface water, soil moisture, snow and glaciers all contribute to GRACE observations, but it is not possible to separate them. Estimates of water storage suffer from measurement errors and noise which are reduced with different filtering approaches (Swenson & Wahr 2002). Data are available from August 2002, approximately every 30 days, even if not always at regular intervals. The spatial resolution is equal to 0.25°. Data have been acquired from http://grace.jpl.nasa.gov.

MODIS evapotranspiration

ET products (MOD16 ET) are estimated using the algorithm developed by Mu *et al.* (2011), which improves the Mu *et al.* (2007) algorithm. ET estimate is based on the Penman–Monteith equation. This dataset is available at global scale at a spatial resolution of 1 km^2 and at different temporal resolutions from 8 days to a month and years from 2000 to 2010. Vegetation information is acquired from the MODIS database, while meteorological information is non-satellite data from NASA's MERRA GMAO daily meteorological reanalysis. An average RMSE of the 8-day latent heat flux product has been computed by comparing MODIS estimates with data from 19 eddy covariance towers in the USA and a value of 29.5 $W\,m^{-2}$ has been reported (Mu *et al.* 2007).

The monthly product at 0.05° of spatial resolution will be used in this work (*ET_MODIS*).

Ground data

Precipitation

Meteorological data of rainfall are available from 1 January 2000 to 31 December 2004 at daily scale from the National Climatic Data Center (NDCD) database (http://www.ncdc.noaa.gov/oa/ncdc.html). In particular, 158 stations are available. These data have been aggregated at monthly scale for each station and then interpolated over the basin with the inverse weight distance method.

Streamflow

Daily discharges data have been analysed at Yichang station (30.66 N, 111.23 E) and aggregated for each month. These data are available from the Global Runoff Data Center which has a database of more than 3,600 stations around the world.

Data from hydrological modelling

The hydrological distributed energy water balance model FEST-EWB (Mancini 1990; Rabuffetti *et al.* 2008; Corbari *et al.* 2009, 2011) is used to compute monthly ET data (*ET_FEST-EWB*).

The core of the model is the system between energy and mass balance equations at the ground surface:

$$\begin{cases} \dfrac{\mathrm{d}SM}{\mathrm{d}t} = \dfrac{P - R - PE - \mathrm{ET}}{\mathrm{d}z} & (1) \\ R_n - G - H - LE = \dfrac{\mathrm{d}S}{\mathrm{d}t} & (2) \end{cases}$$

where SM (–) is the soil water content, ET (mm) is the ET, P (mm) is the precipitation rate, R (mm) is the runoff flux, PE (mm) is the drainage flux, $\mathrm{d}z$ (mm) is the soil depth, R_n (Wm^{-2}) is the net radiation, G (Wm^{-2}) is the soil heat flux, H (Wm^{-2}) is the sensible heat flux, LE (Wm^{-2}) is the latent heat flux, $\mathrm{d}S/\mathrm{d}t$ encloses the energy storage terms. These equations are solved explicitly with respect to the representative equilibrium temperature of the pixel (*RET*) that is the land surface temperature which closes the energy balance.

In particular, ET is linked to the latent heat flux through the latent heat of vaporisation (λ) and the water density (ρ_w):

$$LE = \lambda \rho_w \mathrm{ET} \quad (3)$$

The latent heat flux is computed as:

$$LE = \frac{\rho_a c_p}{\gamma}(e^* - e_a)\left[\frac{f_v}{(r_a + r_c)} + \frac{1 - f_v}{(r_{abs} + r_s)}\right] \quad (4)$$

where ρ_a is the air density, γ is the psychometric constant ($\mathrm{Pa}^{\circ}\mathrm{C}^{-1}$), f_v is the vegetation fraction and c_p is specific heat of humid air ($\mathrm{MJkg}^{-1}\,\mathrm{K}^{-1}$). The saturation vapour pressure (e^*) is computed as a function of the *RET* while the vapour pressure (e_a) is computed as a function of air temperature. The canopy resistance (r_c) is expressed following Jarvis (1976), while the soil resistance (r_s) is according to Sun (1982). The aerodynamic resistance (r_a for vegetation and r_{abs} for bare soil) is computed using the Thom model (Thom 1975).

Runoff is computed according to a modified Soil Conservation Service-Curve Number (SCS-CN) method extended for continuous simulation (Ravazzani *et al.* 2008) where the potential maximum retention is updated cell by cell at the beginning of rainfall as a linear function of the degree of saturation; while its routing throughout the hillslope and the river network is performed using the Muskingum-Cunge method in its non-linear form with the time variable celerity (Montaldo *et al.* 2007).

This model has been extensively calibrated and validated in each algorithm module at different spatial and temporal scales: the snow dynamic by Corbari *et al.* (2009), where the accumulation and melting processes have been calibrated using snow coverage images from MODIS; the runoff routing by Montaldo *et al.* (2007) and Rabuffetti *et al.* (2008); the groundwater dynamic by Ravazzani *et al.* (2011). The coupled system of the energy and mass balance equation has been calibrated in an innovative way using land surface temperature data from remote sensing for model internal calibration as a complementary method to the traditional discharge measurements. This approach offers the possibility to control ET fluxes at pixel scale, opening up a new vision to control the mass balance not based only on the discharge measures (generally few at the basin scale), but also on ET fluxes in any pixel in which the basin surface is discretised. This approach has been tested at local scale for a maize field in Landriano (Italy), at the agricultural district scale for Barrax (Spain) and for the Upper Po River basin (Italy) showing a good ability of the model in reproducing the observed *LST* values in terms of mean bias error, root mean square error (RMSE), relative error and Nash and Sutcliffe index (Corbari *et al.* 2010, 2011, 2013).

The FEST-EWB model has also been calibrated for the Upper Yangtze River basin (Corbari *et al.* 2012) comparing *LST* from MODIS and simulated land surface temperature. Meteorological input data of rainfall, air temperature, relative air humidity and horizontal wind velocity are available from 1 January 2000 to 31 December 2004 from the NDCD database. The model was run at a spatial resolution of 5 km from 2000 to 2004 at hourly scale. Model outputs are ET maps, discharge and also water storage derived from the joint contribution of snow and groundwater.

METHODOLOGY

ET is estimated as the residual term of the water balance equation as:

$$\mathrm{ET} = P - Q - \Delta S \tag{5}$$

where ET is evapotranspiration (mm day^{-1}), P is precipitation which encloses rainfall and snowfall (mm day^{-1}), Q is surface and subsurface discharge (mm day^{-1}) and ΔS is the change of water storage where ground water, snow and glacier are all included (mm day^{-1}).

Two different ET estimates are retrieved: (1) using as input ground precipitation data (*ET_pluv*) and (2) using as input satellite precipitation data (*ET_TRMM*).

Following the methodology proposed by Rodell *et al.* (2004), the relative error for ET is then computed as:

$$\varepsilon_{\overline{\mathrm{ET}}} = \sqrt{\frac{\varepsilon_{\overline{P}}^2 \overline{P^2} + \varepsilon_{\overline{Q}}^2 \overline{Q^2} + \varepsilon_{\overline{\Delta S}}^2 \overline{\Delta S^2}}{\bar{P} - \bar{Q} - \overline{\Delta S}}} \tag{6}$$

where ε is the relative uncertainty computed for each component of the water cycle, while $\overline{P}$, $\overline{Q}$, $\overline{\Delta S}$ are the mean values. This equation is applicable only if the errors of each single component are independent and normally distributed.

Comparison strategy

The ET estimates are computed at the spatial and temporal scales of GRACE observations, which are the more restrictive conditions. Thus the different information, satellite data and modelled outputs, are resampled to 0.25° of pixel dimension and monthly averaged. To be more precise, GRACE observations are not always available at regular intervals, so that the average period is changeable between 28 and 31 days. The comparisons are performed from September 2002 to December 2004.

Goodness of models and remote sensing estimates is evaluated through different statistical indexes: the mean bias error (MBE), the RMSE and the absolute error (ARE), which are computed as follows:

$$\mathrm{MBE} = \frac{\sum_{i=1}^{n} \left(X_{\mathrm{sim}}^i - X_{\mathrm{obs}}^i\right)}{n} \tag{7}$$

$$\mathrm{RMSE} = \left[\frac{\sum_{i=1}^{n} \left(X_{\mathrm{sim}}^i - X_{\mathrm{obs}}^i\right)^2}{n}\right]^{0.5} \tag{8}$$

$$\mathrm{ARE} = 100 \cdot \frac{\sum_{i=1}^{n} \left|\frac{X_{\mathrm{sim}}^i - X_{\mathrm{obs}}^i}{X_{\mathrm{obs}}^i}\right|}{n} \tag{9}$$

where ${X_{\mathrm{sim}}}^{i\mathrm{th}}$ is the ith simulated variable by FEST-EWB, ${X_{\mathrm{obs}}}^{i\mathrm{th}}$ is the ith measured variable, n the sample size and $\overline{X_{\mathrm{obs}}}$ the average observed variable.

The spatial variability of ET, water storage and precipitation is also investigated studying the mutual relationship between parameters' values in each pixel. The relationship between different pixel values at a defined distance is computed with the spatial autocorrelation function (AC):

$$AC(d_{1,2}) = \frac{E\{[\mathrm{par}(X_1) - \mu] * [\mathrm{par}(\mathrm{X}_2) - \mu]\}}{\sigma^2} \tag{10}$$

where μ is the mean and σ^2 is the variance of the parameter (par) in stationary hypothesis, so that a stochastic process, whose joint probability distribution does not change in time or space, is considered. x_1 and x_2 are the generic positions at a fixed distance d. The autocorrelation function should be studied under isotropy hypothesis so that d is a function only of the distance between two points and not of the direction.

RESULTS

In the following paragraphs, the remotely sensed products of precipitation and water storage are compared with ground data and simulation outputs; as well, ET from the simplified procedure of the closure of water balance is compared to the distributed hydrological model results in order to understand whether this simple approach can be used when few ground data are available.

Precipitation

The comparison between monthly rainfall estimates from TRMM and from ground rain gauges is performed. In Figure 2, as an example, images from TRMM and ground

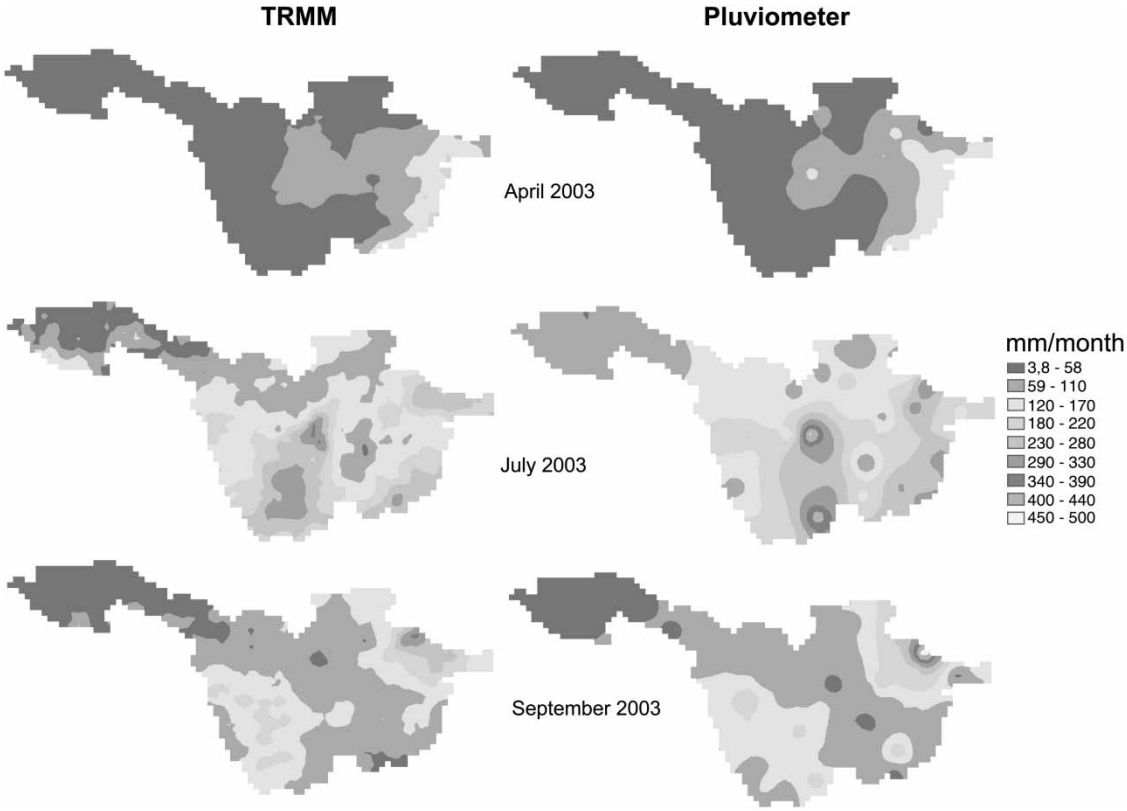

Figure 2 | Comparison between monthly TRMM and ground data for the example dates of April 2003, July 2003 and September 2003.

data are reported for April 2003 during the dry season, and for July and September 2003 for the rainy season. A good agreement is visible in terms of monthly values and also of spatial distributions. Spatial autocorrelation functions are then computed for these three selected dates and, in Figure 3, AC values are reported as a function of distance for ground and satellite data. The three couples of autocorrelation functions have a similar shape. Moreover, as expected, AC values are equal to 1 at a 0° distance and decrease to values near zero as the distance between the two pixels increases.

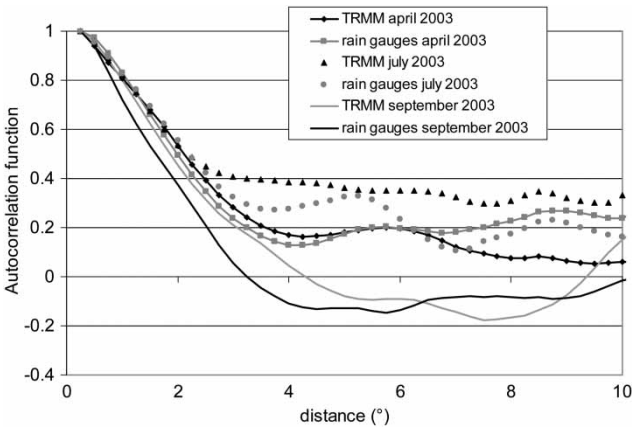

Figure 3 | Spatial autocorrelation functions of precipitation for TRMM and ground data for the examples dates of April 2003, July 2003 and September 2003.

These results in agreement are confirmed from the statistical analyses, which are reported in Table 1, showing MBE, RMSE and ARE. MBE between ground measured data minus satellite images for the 28 selected months is equal to 18 mm with a standard deviation of 19.6 mm. In fact, ARE is equal to 5.2% and RMSE to 64.6 mm. In Figure 4, the spatial means of each image from satellite and from interpolated ground data are reported showing similar monthly values. These results indicate a good accordance between satellite and ground data considering also the errors related to the measures. Precipitation uncertainty has been assumed equal to 11% according to Rodell *et al.* (2004). These analyses confirm the results found by Huffman *et al.* (2007), which state that these satellite rainfall products provide good performance at monthly scale while lesser skill is highlighted for short flood events.

Table 1 | Statistical analysis for precipitation, water storage and discharge data

		Entire database	Period$_1$	Period$_2$
Precipitation	MBE (mm day^{-1})	− 0.30	− 0.20	− 0.49
	RMSE (mm day^{-1})	0.39	0.06	0.33
	ARE (%)	5.2	9.6	2.7
Water storage	MBE (mm day^{-1})	− 0.11	0.05	− 0.42
	RMSE (mm day^{-1})	1.20	0.85	2.56
	ARE (%)	20	16.8	23.1
Discharge	MBE (mm day^{-1})	0.11	0.14	0.06
	RMSE (mm day^{-1})	0.41	0.11	0.26
	ARE (%)	19	21.1	15.1

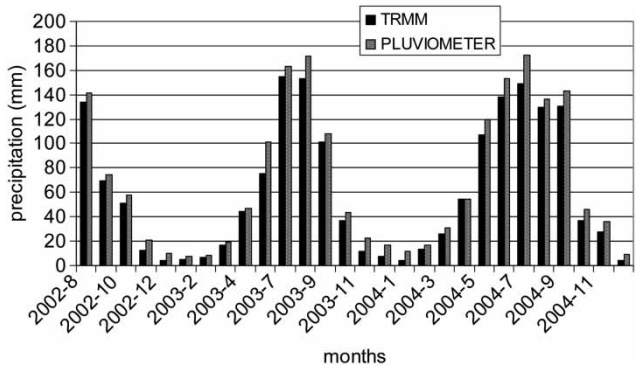

Figure 4 | Monthly mean and spatially averaged values of precipitation from satellite and ground data and their variance.

Table 2 | Statistical analysis for ET data

		Entire database	Period$_1$	Period$_2$
ET_PLUV vs *ET_TRMM*	MBE (mm day^{-1})	0.34	0.49	0.20
	RMSE (mm day^{-1})	0.39	0.33	0.06
	ARE (%)	51.4	25.6	65.1
ET_PLUV vs *ET_FEST-EWB*	MBE (mm day^{-1})	0.20	0.30	0.05
	RMSE (mm day^{-1})	1.18	1.12	0.74
	ARE (%)	66.0	77.4	57.0
ET_MODIS vs *ET_FEST-EWB*	MBE (mm day^{-1})	1.37	1.34	1.39
	RMSE (mm day^{-1})	1.38	1.82	1.97
	ARE (%)	55.5	40.2	63.7

The Upper Yangtze River basin area is characterised by a typical monsoon climate with strong heavy rain during summer and a dry winter (Figure 4). Thus an intercomparison between ground and satellite data is performed by distinguishing between the period of May to September (period$_1$) with mean values above 80 mm month^{-1} and from October to April (period$_2$) with mean rainfall less than 80 mm month^{-1}. ARE for period$_1$ is equal to 9.6% which is higher than for period$_2$ when ARE is 2.7%. In this winter period$_2$, the measures both from ground and satellite are also influenced by the snowfall which increases errors variability, even though low precipitation occurs.

Water storage

Ground and surface water, soil moisture, snow and glacier all contribute to GRACE observations, but they cannot be separated. GRACE data have an absolute error of 25 mm between two subsequent observations which are needed to calculate the change in water storage (Tapley *et al.* 2004). In Figure 5, monthly mean and spatially averaged values of water storage from satellite and modelling data are reported for the whole period of analysis. A general mean difference between GRACE minus FEST-EWB is equal to −0.1 mm day^{-1} with a standard deviation of 1.2 mm day^{-1}. ARE is equal to 20% and RMSE to 1.2 mm day^{-1}. Negative differences between FEST-EWB minus GRACE are found during winter periods with positive values during summer, as reported in Table 1. Some discordant results in terms of sign are obtained from GRACE measurements with respect to the hydrological model outputs. For example, during March 2003, FEST-EWB water storage is equal to −0.55 mm day^{-1} while GRACE value is 1.44 mm day^{-1}.

A good spatial agreement between satellite and modelled water storage is highlighted in Figure 6 where the spatial autocorrelation functions for the selected dates of April 2003, July 2003 and September 2003 are reported for GRACE and FEST-EWB models. During July 2003, higher AC values are found, in accordance with the results obtained for precipitation analysis.

Streamflow

In Figure 7 the comparison between observed and simulated monthly discharges is reported and a good agreement is shown. In particular, the mean difference is equal to 0.1 mm day^{-1} with a standard deviation of 0.4 mm day^{-1};

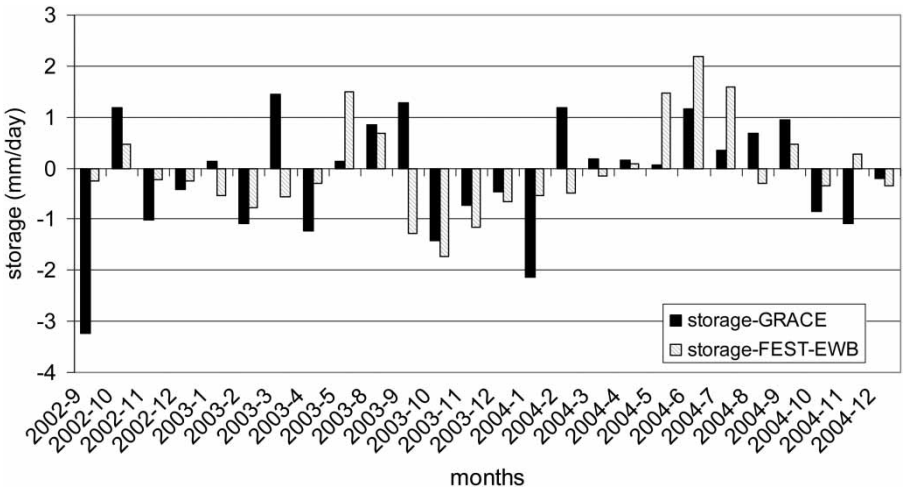

Figure 5 | Monthly mean and spatially averaged values of water storage from satellite and modelling data.

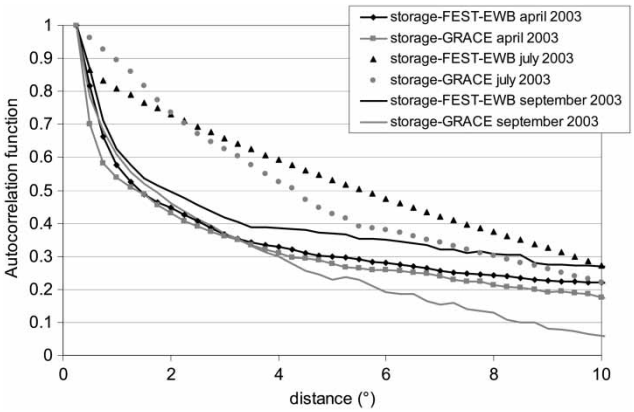

Figure 6 | Spatial autocorrelation functions for water storage from GRACE and from FEST-EWB model for the examples dates of April 2003, July 2003 and September 2003.

while ARE is equal to 19% and RMSE to 0.41 mm day^{-1}. A higher relative error is found during period$_1$, when streamflow is significant, than during period$_2$ (Table 1).

These errors are relatively small according also to the high uncertainty which affects ground river flow data. In fact, Pelletier (1987), after reviewing 140 publications on river discharge errors, found that the uncertainty ranges between 8 and 20%. Di Baldassarre & Montanari (2009) highlighted that errors along the River Po (Italy) are in between 6.2 and 42.8%. The authors did not find any errors related to the Yangtze River discharge in the literature, but supported by literature analysis, an error of about 20% should be taken into account.

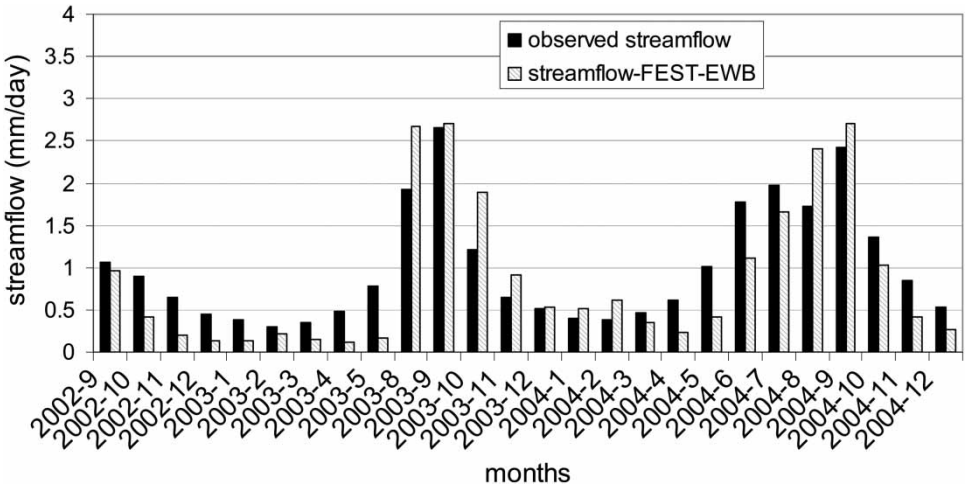

Figure 7 | Monthly mean values of streamflow from ground and modelling data.

Evapotranspiration

In Figure 8 monthly ET values computed as a residual term of the water budget using TRMM data and ground rainfall data are compared to the ET simulated from FEST-EWB and to the MODIS ET product. ET estimates using ground precipitation data have higher monthly values than *ET_TRMM* with a mean difference of 0.34 mm day^{-1}, a standard deviation of 0.25 mm day^{-1} and a RMSE of 0.39 mm day^{-1}. These results are in agreement with the differences found in terms of rainfall, where rain gauges overestimate satellite data (Figure 4 and Table 1). Instead, if *ET_pluv* and *ET_FEST-EWB*, which are forced with the same precipitation data, are compared, a mean difference of 0.20 mm day^{-1} is found with a standard deviation of 1.19 mm day^{-1} and RMSE of 1.18 mm day^{-1}. The wetter period is also characterised by a high difference in terms of *ET*; in fact, RMSE between *ET_PLUV* and *ET_TRMM* is equal to 0.33 mm day^{-1} for period$_1$ and 0.06 mm day^{-1} for period$_2$, while RMSE between *ET_FEST-EWB* and *ET_PLUV* is equal to 1.12 mm day^{-1} for period$_1$ and 0.74 for period$_2$.

During some months, the computed ET as a residual term of the energy balance (*ET_pluv* and *ET_TRMM*) becomes negative, which cannot be feasible. These anomalies are obtained during winter periods, which can be related to an erroneous simulation of the snow dynamic from GRACE data. If, for example, March 2003 is considered, monthly precipitation from TRMM and ground data are in accordance with similar mean values of 16.9 and 19.4 mm, respectively. The only discrepancy is found in water storage data where GRACE has a positive value of 36.8 mm, while FEST-EWB estimate is negative and equal to –17.0 mm. A similar combination is found also for the other months where *ET_pluv* and *ET_TRMM* are negative.

When ET from MODIS is compared to the other three previous ET estimates, a considerable overestimation is found for each month (Figure 8). This result is confirmed from the error statistics computed against modelled ET from FEST-EWB. In fact, a MBE of 1.37 mm day^{-1} and a RMSE of 1.38 mm day^{-1} are found. Moreover, no variability in terms of errors is highlighted during the wet or dry season and this effect can be seen as a constant bias between MODIS ET product and the other three ET estimates analysed in this paper. Mu *et al.* (2011) compared *ET_MODIS* with eddy covariance stations over different vegetation coverage in the USA, reporting an overall mean absolute error of 24.1%, which is lower with respect to the ARE found in this work over the Upper Yangtze River basin when *ET_FEST-EWB* is equal to 55%.

Ramillien *et al.* (2006) computed monthly ET for the Yangtze River basin using different global models and ground and satellite data. During the winter period ET is

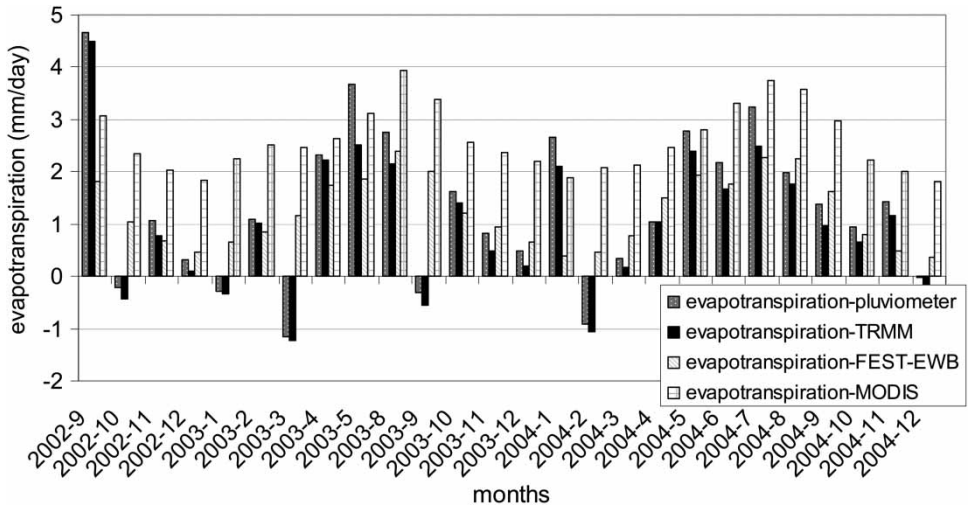

Figure 8 | Comparison between residual ET using satellite and ground data and ET from the FEST-EWB model and ET from MODIS.

generally lower than 1 mm day^{-1}, which is in accordance with *ET_FEST_EWB*, *ET_pluv* and *ET_TRMM* while *ET_MODIS* reaches higher values. During the monsoon season, higher variability in ET estimates is highlighted by Ramillien *et al.* (2006), with values between 2.5 and 4 mm day^{-1} which can enclose the bias between MODIS and FEST-EWB data.

In Figure 9, the autocorrelation functions for the three selected dates of April 2003, July 2003 and September 2003 are reported for *ET_FEST-EWB* and *ET_MODIS*. During the different months, the pairs of curves behave the same way confirming the ability of the two ET estimates to correctly reproduce the spatial variability.

According to Equation (6), the contribution of each component to the overall error in the ET residual estimates has also been analysed in order to understand how each term of the water budget influences the estimate of ET. The overall error on *ET_TRMM* estimates for each month is computed and a mean value of error equal to 0.6 mm day^{-1} is found. If $\varepsilon_{\overline{ET}}$ for *ET_pluv* is computed, a mean value of 0.4 mm day^{-1} is obtained.

DISCUSSION AND CONCLUSIONS

The present work analysed the possibility to estimate ET from ground and satellite data using the simple water balance equation for the Upper Yangtze River basin from 2002 to 2004 at monthly scale. Precipitation data have been retrieved from TRMM satellite and compared with spatial distributed ground data showing an underestimation of 18 mm with a standard deviation of 19.6 mm. Water storage has been analysed from GRACE satellite data and the highest uncertainties have been found to affect this water budget component.

ET has been calculated as the residual term of the water balance equation and error statistics have been computed in comparison to a distributed energy water balance model. A general good agreement between them has been found with a mean bias of 0.07 ± 1.19 mm day^{-1} at monthly scale. However, during some months, residual ET, *ET_TRMM* and *ET_pluv* becomes negative which cannot be feasible. Thus ET data using only satellite data seem to be still not operative, in particular for engineering and environmental applications as parsimonious irrigation, real-time flood forecast and quantitative water resources availability where higher spatial and temporal resolutions as well as more accurate estimates are needed. Remote sensing products still have relevant retrieval errors and the highest uncertainties seem to be confined in GRACE estimates which are also the most difficult data to validate with ground information. These errors are then, of course, reflected in ET estimates which tend to be higher then modelled values. Moreover, discrepancies between temporal and spatial resolutions are still present among the different hydrology products from satellite. In fact, GRACE data have a clearly coarser resolution with respect to the other information leading to possible pixel inconsistencies.

Furthermore, the Yangtze River basin is a quite huge basin with different climatic, hydrologic and ecosystem characteristics which determine different parameters in the algorithm estimations of the different hydrological variables. Of course, also the hydrological model, even if calibrated and validated, can include some errors in its parameterisation.

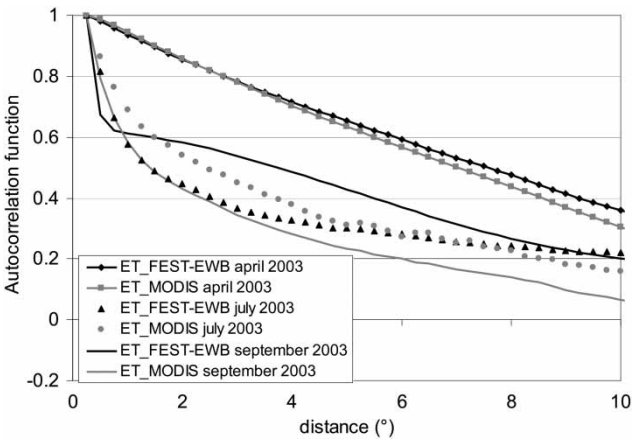

Figure 9 | Spatial autocorrelation functions for ET from MODIS and from FEST-EWB model for the examples dates of April 2003, July 2003 and September 2003.

ACKNOWLEDGEMENTS

This work was supported in the framework of the Dragon 2 Programme between the European Space Agency (ESA) together with the National Remote Sensing Centre of China (NRSCC).

REFERENCES

Adler, R., Wilheit, J. R., Kummerow, C. & Ferraro, R. 2007 *AMSR-E/Aqua L2B Global Swath Rain Rate/Type GSFC Profiling Algorithm V002*. National Snow and Ice Data Center. Digital media, Boulder, Colorado, USA.

Anderson, M. C., Norman, J. M., Diak, G. R., Kustas, W. P. & Mecikalski, J. R. 1997 A two-source time-integrated model for estimating surface fluxes using thermal infrared remote sensing. *Remote Sens. Environ*. **60**, 195–216.

Bastiaanssen, W. G. M., Menenti, M., Feddes, R. A. & Holtslag, A. A. M. 1998 A remote sensing surface energy balance algorithm for land (SEBAL) 1. Formulation. *J. Hydrol*. **212–213**, 198–212.

Birkett, C. M. 1998 Contribution of the TOPEX NASA radar altimeter to the global monitoring of large rivers and wetlands. *Water Resour. Res*. **34** (5), 1223–1239.

Corbari, C., Mancini, M., Li, J. & Su, Z. 2012 Can satellite land surface temperature data be used similarly to ground discharge measurements for distributed hydrological model calibration? (submitted to *Hydrological Science Journal*).

Corbari, C., Ravazzani, G. & Mancini, M. 2011 A distributed thermodynamic model for energy and mass balance computation: FEST-EWB. *Hydrol. Process*. **25**, 1443–1452.

Corbari, C., Ravazzani, G., Martinelli, J. & Mancini, M. 2009 Elevation based correction of snow coverage retrieved from satellite images to improve model calibration. *Hydrol. Earth Syst. Sci*. **13**, 639–649.

Corbari, C., Sobrino, J. A., Mancini, M. & Hidalgo, V. 2010 Land surface temperature representativeness in a heterogeneous area through a distributed energy-water balance model and remote sensing data. *Hydrol. Earth Syst. Sci*. **14**, 2141–2151.

Corbari, C., Sobrino, J. A., Mancini, M. & Hidalgo, V. 2013 Mass and energy fluxes estimates at different spatial resolutions in a heterogeneous area through a distributed energy-water balance model and remote sensing data. *Int. J. Remote Sens*. **34** (9–10), 3208–3230.

Crow, W. T., Wood, E. F. & Pan, M. 2003 Multiobjective calibration of land surface model evapotranspiration predictions using streamflow observations and spaceborne surface radiometric temperature retrievals. *J. Geophys. Res. – Atmos.* **108** (D23).

Di Baldassarre, G. & Montanari, A. 2009 Uncertainty in river discharge observations: a quantitative analysis. *Hydrol. Earth Syst. Sci*. **13**, 913–921.

Frappart, F., Calmant, S., Cauhope, M., Seyler, F. & Cazenave, A. 2006 Preliminary results of ENVISAT RA-2-derived water levels validation over the Amazon basin. *Remote Sens. Environ*. **100**, 252–264.

Gao, H., Tang, Q., Ferguson, C. R., Wood, E. F. & Lettermaier, D. P. 2010 Estimating the water budget of major US river basins via remote sensing. *Int. J. Remote Sens*. **31** (14), 3955–3978.

Jarvis, P. G. 1976 The interpretation of the variations in leaf water potential and stomatal conductance found in canopies in the field. *Philos. T. Roy. Soc. B* **273**, 593–610.

Jiménez, C., Prigent, C., Mueller, B., Seneviratne, S. I., McCabe, M. F., Wood, E. F., Rossow, W. B., Balsamo, G., Betts, A. K., Dirmeyer, P. A., Fisher, J. B., Jung, M., Kanamitsu, M., Reichle, R. H., Reichstein, M., Rodell, M., Sheffield, J., Tu, K. & Wang, K. 2011 Global intercomparison of 12 land surface heat flux estimates. *J. Geophys. Res*. **116**, D02102.

Huffman, G. J., Bolvin, D. T., Nelkin, E. J., Wolff, D. B., Adler, R. F., Gu, G., Hong, Y., Bowman, K. P. & Stocker, E. F. 2007 The TRMM Multisatellite Precipitation Analysis (TMPA): Quasi-global, multiyear, combined-sensor precipitation estimates at fine scales. *J. Hydrometeorol*. **8**, 38–55.

Li, X. H., Zhang, Q. & Xu, C.-Y. 2012 Suitability of the TRMM satellite rainfalls in driving distributed hydrological model for water balance computations in Xinjiang catchment, Poyang lake basin. *J. Hydrol*. **426–427**, 28–38.

Mancini, M. 1990 La modellazione distribuita della risposta idrologica: effetti della variabilità spaziale e della scala di rappresentazione del fenomeno dell'assorbimento. PhD thesis, Politecnico di Milano, Milan, Italy (in Italian). (Distributed modelling of the hydrological response: spatial variability effects and representative scale of the absorption process.)

McCabe, M. F., Wood, E. F., Wójcik, R., Pan, M., Sheffield, J., Gao, H. & Su, H. 2008 Hydrological consistency using multi-sensor remote sensing data for water and energy cycle studies. *Remote Sens. Environ*. **112**, 430–444.

Moiwo, J. P., Yang, Y., Yanb, N. & Wu, B. 2011 Comparison of evapotranspiration estimated by ETWatch with that derived from combined GRACE and measured precipitation data in Hai River Basin, North China. *Hydrolog. Sci. J*. **56** (2), 249–267.

Montaldo, N., Ravazzani, G. & Mancini, M. 2007 On the prediction of the Toce alpine basin floods with distributed hydrologic models. *Hydrol. Process*. **21**, 608–621.

Mu, Q., Heinsch, F. A., Zhao, M. & Running, S. W. 2007 Development of a global evapotranspiration algorithm based on MODIS and global meteorology data. *Remote Sens. Environ*. **111**, 519–536.

Mu, Q., Zhao, M. & Running, S. W. 2011 Improvements to a MODIS global terrestrial evapotranspiration algorithm. *Remote Sens. Environ*. **115**, 1781–1800.

Norman, J. M., Kustas, W. P. & Humes, K. S. 1995 Source approach for estimating soil and vegetation energy fluxes in observations of directional radiometric surface temperature. *Agric. Forest Meteor*. **77**, 263–293.

Oki, T. & Kanae, S. 2006 Global hydrological cycles and world water resources. *Science* **313** (5790), 1068–1072.

Pan, M. & Wood, E. F. 2006 Data assimilation for estimating the terrestrial water budget using a constrained ensemble Kalman filter. *J. Hydrometeor*. **7**, 534–547.

Pelletier, M. P. 1987 Uncertainties in the determination of river discharge: a literature review. *Can. J. Civil Eng*. **15**, 834–850.

Rabuffetti, D., Ravazzani, G., Corbari, C. & Mancini, M. 2008 Verification of operational Quantitative Discharge Forecast (QDF) for a regional warning system – the AMPHORE case studies in the upper Po River. *Nat. Hazard. Earth Syst.* **8**, 1–13.

Ramillien, G., Frappart, F., Güntner, A., Ngo-Duc, T., Cazenave, A. & Laval, K. 2006 Time variations of the regional evapotranspiration rate from Gravity Recovery and Climate Experiment (GRACE) satellite gravimetry. *Water Resour. Res.* **42**, W10403.

Ravazzani, G., Rabuffetti, D., Corbari, C. & Mancini, M. 2008 Validation of FEST-WB, a continuous water balance distributed model for flood simulation. In: *Proceedings of XXXI Italian Hydraulic and Hydraulic Construction Symposium*, Perugia, Italy.

Ravazzani, G., Rametta, D. & Mancini, M. 2011 Macroscopic cellular automata for groundwater modelling: a first approach. *Environ. Modell. Softw.* **26** (5), 634–643.

Rodell, M., Famiglietti, J. S., Chen, J., Seneviratne, S. I., Viterbo, P., Holl, S. & Wilson, C. R. 2004 Basin scale estimates of evapotranspiration using GRACE and other observations. *Geophys. Res. Lett.* **31**, L20504.

Roux, E., Cauhope, M., Bonnet, M. P., Calmant, S., Vauchel, P. & Seyler, F. 2008 Daily water stage estimated from satellite altimetric data for large river basin monitoring. *Hydrolog. Sci. J.* **53** (1), 81–89.

Sheffield, J., Ferguson, C., Troy, T., Wood, E. F. & McCabe, M. 2009 Closing the terrestrial water budget from satellite remote sensing. *Geophys. Res. Lett.* **36** (7).

Su, Z. 2002 The Surface Energy Balance System (SEBS) for estimation of turbulent heat fluxes. *Hydrol. Earth Syst. Sci.* **6** (1), 85–100.

Sun, S. F. 1982 Moisture and Heat Transport in a Soil Layer Forced by Atmospheric Conditions. MSc Thesis, University of Connecticut, Storrs, CT.

Swenson, S. & Wahr, J. 2002 Methods for inferring regional surface-mass anomalies from GRACE measurements of timevariable gravity. *J. Geophys. Res.* **107**, 2193.

Tapley, B. D., Bettadpur, S., Watkins, M. & Reigber, C. H. 2004 The gravity recovery and climate experiment; mission overview and early results. *Geophys. Res. Lett.* **31**, L09607.

Thom, A. S. 1975 Momentum, mass and heat exchange of plant communities. In: *Vegetation and Atmosphere* (J. L. Monteith, ed.). Academic Press, London, pp. 57–110.

First received 7 January 2013; accepted in revised form 6 August 2013. Available online 12 September 2013